

Subfamily-Specific Fluorescent Probes for Cysteine Proteases Display Dynamic Protease Activities during Seed Germination¹

Haibin Lu, Balakumaran Chandrasekar, Julian Oeljeklaus, Johana C. Misas-Villamil, Zheming Wang, Takayuki Shindo, Matthew Bogyo, Markus Kaiser, and Renier A.L. van der Hoorn*

Plant Chemetics Laboratory, Department of Plant Sciences, University of Oxford, Oxford OX1 3RB, United Kingdom (H.L., B.C., J.C.M.-V., R.A.L.v.d.H.); Plant Chemetics Laboratory, Max Planck Institute for Plant Breeding Research, 50829 Cologne, Germany (H.L., B.C., J.C.M.-V., T.S., R.A.L.v.d.H.); Center for Medical Biotechnology, Faculty of Biology, University of Duisburg-Essen, 45117 Essen, Germany (J.O., Z.W., M.K.); and Department of Pathology, Stanford School for Medicine, Stanford, California 94305–5324 (M.B.)

Cysteine proteases are an important class of enzymes implicated in both developmental and defense-related programmed cell death and other biological processes in plants. Because there are dozens of cysteine proteases that are posttranslationally regulated by processing, environmental conditions, and inhibitors, new methodologies are required to study these pivotal enzymes individually. Here, we introduce fluorescence activity-based probes that specifically target three distinct cysteine protease subfamilies: aleurain-like proteases, cathepsin B-like proteases, and vacuolar processing enzymes. We applied protease activity profiling with these new probes on *Arabidopsis* (*Arabidopsis thaliana*) protease knockout lines and agroinfiltrated leaves to identify the probe targets and on other plant species to demonstrate their broad applicability. These probes revealed that most commercially available protease inhibitors target unexpected proteases in plants. When applied on germinating seeds, these probes reveal dynamic activities of aleurain-like proteases, cathepsin B-like proteases, and vacuolar processing enzymes, coinciding with the remobilization of seed storage proteins.

Cys proteases are a large class of proteolytic enzymes that carry a catalytic Cys residue in the active site. Plant genomes encode more than 100 Cys proteases that act in the cytoplasm, the endomembrane system, and the apoplast (Beers et al., 2004; García-Lorenzo et al., 2006; van der Hoorn, 2008; Martínez et al., 2012). Well-studied Cys proteases include different papain-like cysteine proteases (PLCPs; family C1A of clan CA), vacuolar processing enzymes (VPEs; family C13 of clan CD), metacaspases (family C14 of clan CD), and multiple families of deubiquitinating enzymes (families 12, 19, and 48 of clans CA and CE).

PLCPs and VPEs have been studied for their role in programmed cell death (PCD), both in immunity and development. Tomato (*Solanum lycopersicum*) Required

for *Cladosporium* Resistance3 and tobacco (*Nicotiana tabacum*) cathepsin B, for example, are PLCPs required for PCD upon pathogen perception (Krüger et al., 2002; Gilroy et al., 2007), while *Arabidopsis* (*Arabidopsis thaliana*) Cysteine Endopeptidase1 and δ VPE are pivotal for developmental PCD in pollen and seed coat development, respectively (Nakaune et al., 2005; Zhang et al., 2014). Likewise, *Arabidopsis* Responsive to Desiccation21 (RD21) is a PLCP required for immunity against *Botrytis cinerea* (Shindo et al., 2012; Lampl et al., 2013), while its *Nicotiana benthamiana* ortholog C14 contributes to immunity against *Phytophthora infestans* (Kaschani et al., 2010; Bozkurt et al., 2011). Suppression of an aleurain-like PLCP delays floret senescence in broccoli (*Brassica oleracea*) and increases susceptibility to pathogens in *N. benthamiana* (Eason et al., 2005; Hao et al., 2006). Furthermore, *Arabidopsis* γ VPE is required for toxin-induced PCD, while its *N. benthamiana* ortholog is required for virus-induced PCD (Hatsugai et al., 2004; Kuroyanagi et al., 2005). In conclusion, these PLCPs and VPEs play different roles, often associated with PCD.

Because of their association with PCD, PLCPs and VPEs are tightly regulated to prevent accidental cell death. Proteases from both families are produced as inactive precursors that require processing in order to remove inhibitory propeptides (Kuroyanagi et al., 2002; Gu et al., 2012). Furthermore, both classes of proteases are tightly regulated by endogenous inhibitors such as cystatins and serpins (Lampl et al.,

¹ This work was supported by the Max Planck Society (European Network Area-Industrial Biotechnology project Produce, COST CM1004 Chemical Proteomics), the University of Oxford, and the European Research Council (starting grant no. 258413 to M.K. and consolidator grant no. 616449, GreenProteases, to R.A.L.v.d.H.).

* Address correspondence to renier.vanderhoorn@plants.ox.ac.uk. The author responsible for distribution of materials integral to the findings presented in this article in accordance with the policy described in the Instructions for Authors (www.plantphysiol.org) is: Renier A.L. van der Hoorn (renier.vanderhoorn@plants.ox.ac.uk).

H.L., B.C., J.C.M.-V., and T.S. performed the experiments; J.O., Z.W., M.B., and M.K. synthesized the probes; R.A.L.v.d.H. wrote the article with input from all authors.

www.plantphysiol.org/cgi/doi/10.1104/pp.114.254466

2013; Zhao et al., 2013). Because of their posttranslational regulations, it is impractical to predict activities of PLCPs and VPEs from transcript abundance.

New, simple, and versatile methods are required to monitor Cys proteases at their activity level in a broad range of plant species. Protease activity profiling (also called activity-based protein profiling of proteases) is an easy and powerful method to monitor the active state of proteases in crude extracts or living organisms (Heal et al., 2011; Serim et al., 2012; Haedke et al., 2013; Willems et al., 2014). Protease activity profiling is based on the use of chemical probes that react covalently with the active site of proteases in an activity-dependent manner. The result of the labeling is a covalent and irreversible bond between the probe and the protease, which allows subsequent separation on protein gels or purification followed by detection by fluorescence scanning or mass spectrometry.

The first probe that we introduced in plant science was DCG-04, which targets PLCPs (van der Hoorn et al., 2004). This probe was subsequently used to monitor PLCP activities during immunity and senescence (Martínez et al., 2007a; Shabab et al., 2008), to study protease activation (Gilroy et al., 2007; Wang et al., 2008; Gu et al., 2012), and to reveal the selectivity of endogenous and pathogen-derived protease inhibitors (Rooney et al., 2005; Tian et al., 2007; Shabab et al., 2008; van Esse et al., 2008; Song et al., 2009; Kaschani et al., 2010; Lampl et al., 2010; Hörger et al., 2012; Lozano-Torres et al., 2012; van der Linde et al., 2012; Mueller et al., 2013; Dong et al., 2014). Although powerful, a disadvantage of DCG-04 profiling is that this biotinylated probe involves an indirect detection using streptavidin-horseradish peroxidase, which reduces throughput and resolution. More recently, we introduced fluorescent versions of DCG-04, coined MV201 and MV202 (Richau et al., 2012), and these probes were used to monitor PLCP activities upon herbicide treatment and during PCD in tomato seedlings (Zulet et al., 2013; Sueldo et al., 2014). Unfortunately, however, MV201 and MV202 can cause severe background labeling, and their targets often cannot be resolved on protein gels because they share the same molecular mass.

More recently, we introduced selective probes for the bacterial effector Avirulence *Pseudomonas syringae* pv. *phaseolicola* protein B (AvrPphB; Lu et al., 2013) and for VPEs (Misas-Villamil et al., 2013). These probes carry selective targeting peptide sequences to improve their selectivity. The AvrPphB probe (FH11) carries an acidic residue at the second amino acid position preceding the cleavage site (P2 = Asp), to mimic substrates of AvrPphB. By contrast, the VPE probe AMS101 carries P2 = Pro to prevent cross-reactivity with PLCPs and P1 = Asn to specifically target VPEs, because these proteases specifically cleave after Asn. These selective probes are much easier to work with and also facilitated in vivo imaging of protease labeling sites. For example, FH11 labeling was used to study the proteolytic activation of AvrPphB in planta,

while AMS101 displayed VPE-specific labeling in the vacuole (Lu et al., 2013; Misas-Villamil et al., 2013).

To speed up plant protease research further, we continue to seek better, more selective probes that target specific proteases. Here, we introduce two new specific probes for two subclasses of PLCPs: aleurain-like proteases (ALPs; subclass 8 of the PLCPs) and cathepsin-like proteases (CTBs; subclass 9 of the PLCPs). We also introduce a new, more readily available probe for VPEs and an improved procedure for PLCP activity profiling with MV202. Using protease mutants, agroinfiltration, virus-induced gene silencing, protease inhibitors, and various plant species, we demonstrate the versatility of these probes and illustrate their applicability by characterizing protease activities during seed germination.

RESULTS

New Probes for Cys Proteases Light Up New Activity Profiles

In this study, we introduce three new probes and improve the analysis of a previously reported probe (Fig. 1A). In addition to the previously used MV202, which targets all PLCPs, we also introduce FY01 and JOGDA1 (Fig. 1A) as selective probes that target a subset of PLCPs. Traditionally, names of activity-based probes bear the two initials of the chemist who synthesized it (M.V., F.Y., or J.O.), followed by a number or recognizable name. MV202 (Richau et al., 2012) is a biotinylated and fluorescent derivative of the protease inhibitor E-64, which carries a Tyr at the P3 position and a Leu at the P2 position, and an epoxide warhead. FY01 was developed in the Bogyo laboratory as a probe for amino dipeptidyl peptidase I/cathepsin C (Yuan et al., 2006). FY01 carries the nonnatural amino acid nor-Val at the P2 position and homo-Phe at the P1 position, followed by a vinyl sulfone reactive group and a bodipy fluorophore.

JOGDA1 is a bodipy-labeled derivative of FH11, a probe designed for AvrPphB, a secreted papain-like type III effector produced by *Pseudomonas syringae* (Lu et al., 2013). We resynthesized FH11 with a stronger bodipy fluorophore to improve the detection of labeled proteins. Besides a bodipy residue, JOGDA1 also carries an AOMK reactive group and a Gly-Asp-Ala tripeptide. The Asp residue at the P2 position in FH11 was originally chosen because AvrPphB cleavage requires Asp at P2 of the substrate, which is unique among PLCPs, which usually prefer a hydrophobic residue at the P2 position of the cleavage site. However, we previously reported that, in addition to AvrPphB, FH11 also labels unidentified plant proteins (Lu et al., 2013). Furthermore, we introduce JOPD1 to target legumains/VPEs (Fig. 1A), which cleave after Asn and Asp residues. We previously introduced the aza-epoxide-based probe AMS101 for legumains/VPEs (Misas-Villamil et al., 2013). AMS101, however,

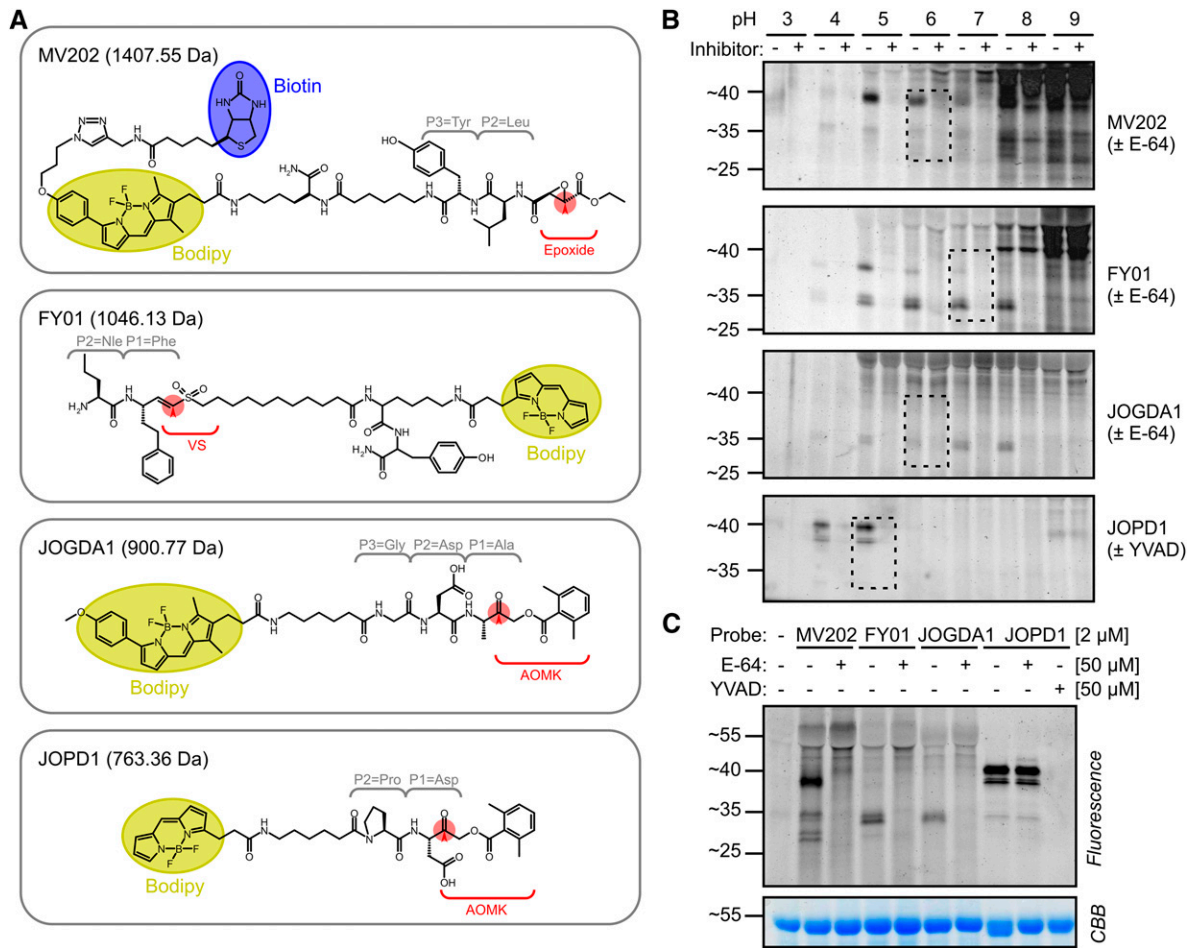


Figure 1. Novel probes display new, pH-dependent labeling profiles. A, Structural components of the novel Cys protease probes. Each of the four probes contains a dipeptide or tripeptide that targets into the P3, P2, and P1 substrate-binding pockets in the different proteases. All probes carry a bodipy fluorescent reporter group (yellow). MV202 also contains a biotin affinity tag (blue). The reactive groups (red) are epoxide, vinyl sulfone (VS), or acyloxymethylketone (AOMK). FY01 carries an N-terminal dipeptide to capture aminodipeptidases. B, Labeling of PLCPs is pH dependent. Leaf extracts were preincubated at pH 3 to 9 with or without 50 μ M E-64/YVAD and then labeled with 2 μ M MV202, FY01, or JOGDA1. Dashed lines indicate selected labeling conditions. C, Comparison of labeling profiles on Arabidopsis leaf extracts. Leaf extracts were preincubated with or without 50 μ M E-64 or Ac-YVAD-cmk and then labeled with 2 μ M probe at pH 5 (JOPD1), pH 6 (MV202 and JOGDA1), or pH 7 (JOPD1). In B and C, samples were separated on protein gels and analyzed by fluorescence scanning and Coomassie Brilliant Blue (CBB) staining.

is synthetically challenging to produce because of the aza-epoxide reactive group. Chemical synthesis of JOPD1 is much less complicated. JOPD1 is a bodipy version of the Pro-Asp-AOMK probe described by Sexton et al. (2007) and carries an Asp at the P1 position, while the Pro at the P2 position prevents the labeling of PLCPs. JOGDA1 and JOPD1 have not been described before, and the details of their synthesis are provided (Supplemental Text S1).

To characterize the targets of MV202, FY01, JOGDA1, and JOPD1, Arabidopsis leaf extracts were labeled at pH 3 to 9 and the labeled proteins were separated on a protein gel and detected by fluorescence scanning. MV202 labeling causes a large number of signals that increase in intensity at higher pH,

especially at pH 8 and 9 (Fig. 1B). Importantly, most labeling is not blocked upon preincubation with E-64, indicating that these signals are not specific. However, clear signals are detected at 25, 35, and 40 kD that are absent upon preincubation with E-64. These signals show an optimum intensity at slightly acidic pH (pH 5–6). pH 6 was chosen for further studies because of the strongest detection of 25- and 35-kD signals.

FY01 labeling causes two close strong signals at 34 kD that are absent upon preincubation with E-64 and have a maximum intensity at neutral pH (pH 6–8; Fig. 1B). At higher pH, unspecific labeling occurs increasingly. This unspecific labeling is less strong at pH 8 when compared with that caused by MV202. FY01 also displays labeling of a specific 40-kD signal at

acidic pH (pH 5), which is presumably identical to the signal caused at 40 kD by MV202. Therefore, we chose pH 7 to display the specific 34-kD signal.

JOGDA1 labeling displays a weak but specific 34-kD signal at pH 5 to 8 (Fig. 1B), which sometimes displays as a doublet on high-resolving protein gels. JOGDA1 labeling causes very low unspecific labeling at higher pH. No other specific signals are displayed with this probe. pH 6 was chosen for further studies, since this caused the strongest labeling in repeated labeling experiments.

Finally, JOPD1 labeling shows signals only at pH 4 and 5 and low unspecific labeling at higher pH (Fig. 1B). The signals consist of two 40-kD signals and a weaker 35-kD signal. Labeling can be prevented upon preincubation with the caspase-1 inhibitor Acetyl-Tyr-Val-Ala-Asp-chloromethylketone (Ac-YVAD-cmk) but not E64 (Fig. 1C). pH 5 was chosen for subsequent labeling experiments, since the signal is strongest at this pH.

A direct comparison of the labeled proteins on one gel shows that the signals have overlapping molecular masses at 40 kD (MV202 and JOPD1) and 34 kD (MV202, FY01, and JOGDA1; Fig. 1C). This figure also shows that unspecific labeling is strongest for MV202, causing strong signals at 40 kD and higher that are not suppressed upon preincubation with E-64.

Improved Broad-Range Fluorescent Profiling of MV202-Labeled Proteomes

The strong, unspecific labeling profile of MV202 was unexpected. MV202 has previously been used only on apoplastic proteomes of tomato and on leaf extracts of agroinfiltrated *N. benthamiana* (Richau et al., 2012; Sueldo et al., 2014). These MV202-labeled proteomes did not show strong background signals, and the few detected signals are specific because they are absent upon preincubation with E-64. We hypothesized that the background labeling is caused by unspecific reaction of the excess MV202 probe when heated up in gel-loading buffer before loading. To test this hypothesis, we labeled leaf proteomes with and without MV202 and then followed three different work-up procedures. Acetone precipitation to remove the excess unlabeled probe does not prevent fluorescent background labeling (Fig. 2A). However, acetone precipitation followed by a purification of biotinylated proteins on avidin beads causes four specific signals of 25 to 30 kD (Fig. 2B). By contrast, purification without acetone precipitation still causes background labeling (Fig. 2C). Taken together, these data indicate that the background labeling is caused by the presence of excess probe that reacts unspecifically with proteins when not removed by precipitation and purification. For the remaining labeling assays with MV202 described in this article, samples were precipitated and purified to prevent background labeling.

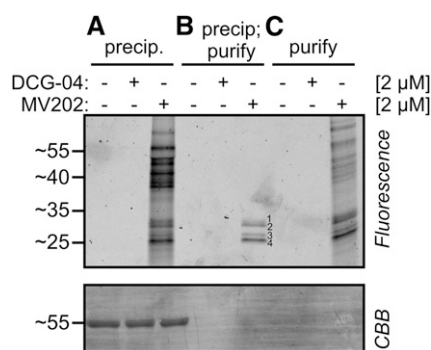


Figure 2. Improved detection by purification of MV202-labeled proteins. Arabidopsis leaf extracts were labeled with and without DCG-04 or MV202. After labeling, the samples were either precipitated in acetone (A), precipitated and purified on avidin beads (B), or directly purified on avidin beads (C). Samples were separated on protein gels and analyzed by fluorescence scanning and Coomassie Brilliant Blue (CBB) staining.

Protease Mutants Identify Different Specific Probe Targets

Because the signals detected by MV202, FY01, and JOGDA1 are blocked by preincubation with E-64 (Fig. 1B), we anticipate that these probes target PLCPs. Likewise, we anticipate that JOPD1 targets legumains/VPEs, because the labeling is blocked upon preincubation with Ac-YVAD-cmk but not E-64 (Fig. 1B). Therefore, we took advantage of Arabidopsis PLCP and VPE mutant collections (Gruis et al., 2004; Wang et al., 2008) to determine the targets of these probes by screening for the absence of labeling. In addition to the single PLCP and VPE mutants, we included double, triple, and quadruple protease mutants. Only protease mutants that show altered labeling profiles are presented here.

Labeling of leaf extracts of protease mutants with MV202 indicated the identity for each of the four signals. The bottom two signals are absent in the *Arabidopsis Aleurain-Like Protein1 (aalp-1)* null mutant (Fig. 3A, signals 3 and 4), indicating that these signals represent AALP. This is consistent with previous data that this region contains the AALP protein upon DCG-04 labeling (van der Hoorn et al., 2004). These bottom signals were also absent in the *aalp-1* mutant using DCG-04 labeling (Gu et al., 2012). Likewise, the top signal (signal 1) is reduced in both the *rd21A-1* and *ctb3-1* mutants (Fig. 3A), indicating that this signal contains RD21 and CTB3, in agreement with previous data where RD21 and CTB3 were identified in this region (van der Hoorn et al., 2004). We believe that the top signal caused an accumulation of both labeled RD21 and CTB3 and not by activation of CTB3 by RD21 or vice versa, because CTB3 labeling is normal in *rd21A-1* mutants (see below) and RD21 processing, accumulation, and activity are unaltered in the *ctb3-1* mutant (Supplemental Fig. S1). The second top signal (signal 2) is absent in the *ctb3-1* mutant (Fig. 3A), indicating that this signal is caused by CTB3.

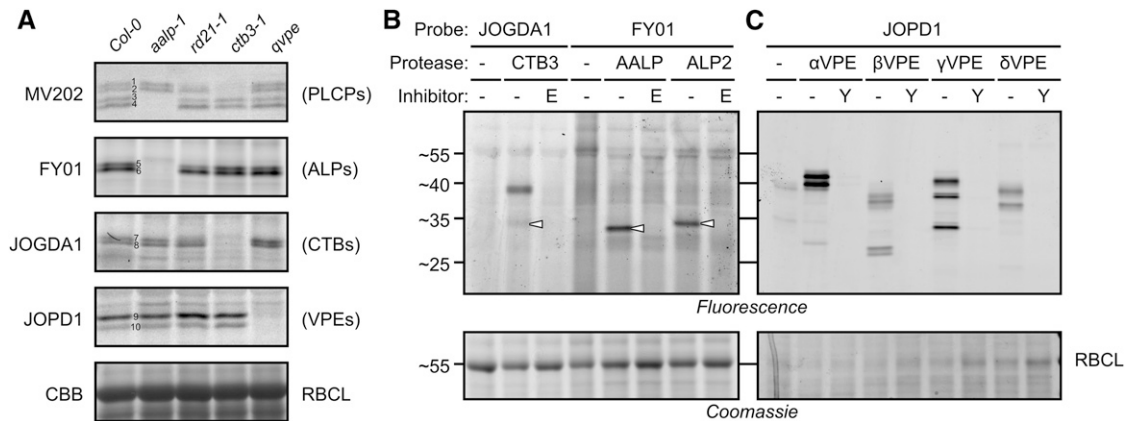


Figure 3. Protease knockout mutants and transient expression reveal specific probe targets in leaf extracts. A, Leaf extracts from wild-type Columbia-0 (Col-0) plants or from *aalp-1*, *rd21-1*, *ctb3-1*, or quadruple *VPE* (*qvpe*) mutants were labeled with MV202, FY01, JOGDA1, or JOPD1 for 3 h under the appropriate labeling conditions. Labeled proteomes were separated on protein gels and analyzed by in-gel fluorescence scanning and Coomassie Brilliant Blue (CBB) staining. B, Extracts of *N. benthamiana* leaves transiently expressing different proteases were preincubated with 50 μ M E-64 (E) and YVAD-cmk (Y) and labeled with FY01, JOGDA1, or JOPD1 with the appropriate labeling conditions. Labeled proteomes were separated on protein gels and analyzed by fluorescence scanning and Coomassie Brilliant Blue staining. RBCL, Rubisco large subunit.

Significantly, labeling of the PLCP mutants revealed that both FY01 signals are absent in the *aalp-1* mutant (Fig. 3A, signals 5 and 6), indicating that FY01 labels AALP. This is surprising, because the molecular mass of the FY01 signals (approximately 34 kD) is larger than the bottom AALP-dependent signals detected upon MV202 labeling (approximately 25 kD; Fig. 3A, signals 3 and 4). Thus, when labeled with FY01, AALP runs at a larger apparent molecular mass than when labeled with MV202, which is opposite to the expected based on the molecular mass of the probes themselves (1 and 1.4 kD, respectively; Fig. 1A). However, selective AALP labeling by FY01 can be explained by the fact that this probe was designed to target aminodipeptidases (Yuan et al., 2006). AALP is a cathepsin H-like aminopeptidase because of the presence of a covalently linked minichain that is retained in the substrate-binding groove to prevent endopeptidase activity (Guncar et al., 1998). The detection of two AALP-dependent FY01 signals is consistent with the earlier observation that AALP accumulates as two mature isoforms on western blots probed with the anti-AALP antibody (Ahmed et al., 2000).

Importantly, the mutant screen also revealed that both signals generated by JOGDA1 labeling are absent in the *ctb3-1* mutant (Fig. 3A, signals 7 and 8), indicating that JOGDA1 targets CTB3. This is also the region where CTB3 has been identified by mass spectrometry (van der Hoorn et al., 2004) and where MV202 labels two CTB3-dependent signals (Fig. 3A, signals 1 and 2). The labeling of CTB3 by JOGDA1 is surprising, since this probe carries an Asp at the P2 position, which was thought to exclude PLCP labeling. To our knowledge, that CTB3 may exist in two isoforms was not reported before.

Finally, to investigate targets for JOPD1, we included the *qvpe* mutant, lacking all four VPEs (Gruis et al., 2004). The JOPD1 signals are absent in this *qvpe* mutant (Fig. 3A, signals 9 and 10), indicating that JOPD1 indeed labels VPEs. This labeling profile is consistent with the occurrence of various active isoforms of γ VPE, the most abundant VPE in leaves (Kuroyanagi et al., 2002; Misas-Villamil et al., 2013). The absence of PLCP labeling by JOPD1 is caused by the fact that PLCPs do not bind peptides with a P2 = Pro residue.

In conclusion, the absence of labeling on mutant plants shows that probe targets are not active in the mutants. At this stage, it is yet unclear if this is caused by the absence of the protease itself or indirectly caused by the removal of a protease that is required to activate the protease that is labeled.

Transient Protease Expression Confirms the Labeling of Respective Proteases

To confirm that the new probes label the different Cys proteases, we transiently expressed CTB3, AALP, ALP2, and all four VPEs by agroinfiltration of *N. benthamiana* and labeled extracts from agroinfiltrated leaves with the respective activity-based probes at the chosen labeling conditions. Specific signals were detected upon labeling of leaves expressing CTB3 with JOGDA1, confirming that JOGDA1 labels CTB3 (Fig. 3B). This signal was absent in leaves where CTB3 was not expressed and in cases where CTB3-containing extracts were preincubated with E-64. The 34-kD signal has the same molecular mass as the CTB3-dependent JOGDA1 signal detected in Arabidopsis leaf extracts, indicating

that the Arabidopsis 34-kD signal originates from CTB3 labeling. Interestingly, an additional, strong 38-kD signal appeared when CTB3-containing extracts were labeled with JOGDA1. This signal was also detected upon MV201 labeling (Richau et al., 2012) and is possibly caused by labeling of the proenzyme of CTB3.

Specific signals were also detected when extracts from leaves transiently expressing AALP and ALP2 were labeled with FY01 (Fig. 3B), confirming that this probe indeed labels both aleurain-like proteases of Arabidopsis. These signals were absent upon preincubation with E-64 and from leaves that do not express AALP or ALP2. Different from the calculated molecular masses of mature AALP and ALP2 proteases (23.7 and 24 kD, respectively), both proteases migrate at larger molecular masses (33 and 34 kD) than expected, and AALP migrates at a slightly lower molecular mass than ALP2. The AALP signal is nevertheless consistent with the AALP-dependent FY01 signal at 34 kD in Arabidopsis leaf extracts, indicating that this signal originates from AALP. ALP2 is not expressed in leaves but is detected in leaves (see below).

Finally, fluorescent signals were also detected when extracts from leaves transiently expressing VPEs were labeled with JOPD1 (Fig. 3C), confirming that all four VPEs can be labeled with JOPD1. These signals are absent upon preincubation with the VPE inhibitor YVAD-cmk and different for extracts not expressing Arabidopsis VPEs, confirming that VPE labeling is specific. The labeling profiles are polymorphic for the different VPEs and consistent with described VPE isoforms and labeling with AMS101 (Kuroyanagi et al., 2012; Misas-Villamil et al., 2013).

In conclusion, these labeling assays on mutant plants and agroinfiltrated leaves show that the three new probes label different subfamilies of Cys proteases: FY01 labels ALPs (e.g. AALP), JOGDA1 targets CTBs (e.g. CTB3), and JOPD1 targets VPEs.

Distinct Protease Activity Profiles in Different Plant Species

To demonstrate that our probes are broadly applicable in plant science, we profiled protease activities in leaf extracts of different (model) plant species, including Solanaceae (winter cherry [*Solanum pseudocapsicum*], tomatillo [*Physalis ixocarpa*], tomato, and tobacco) and monocots (barley [*Hordeum vulgare*] and maize [*Zea mays*]). Preincubation with E-64 or YVAD-cmk was used to demonstrate the specificity of labeling. Detection of fluorescently labeled proteins from protein gels revealed specific signals in all leaf extracts and with all probes that are absent upon preincubation with the respective inhibitors (Fig. 4, A–D), illustrating that labeling with our new probes is broadly applicable. The profiles, however, are remarkably different in molecular mass and intensities. These differences are probably caused by different numbers of protease

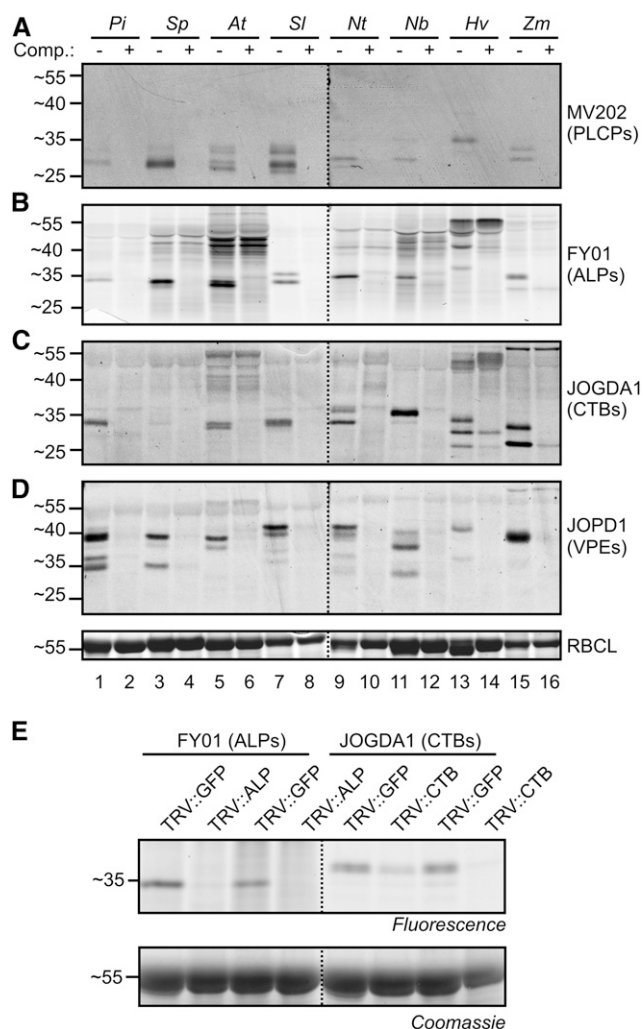


Figure 4. Labeling leaves of different plant species illustrates broad applicability. A to D, Leaf extracts were generated and preincubated with 50 μM (A and B) or 100 μM (C) E-64 or 50 μM JOGDA2 for 30 min and then labeled with 2 μM MV202 (A), FY01 (B), or JOPD1 (D) or 5 μM JOGDA1 (C) for 3 h. Proteins were separated on protein gels, scanned for fluorescence, and stained with Coomassie Brilliant Blue. *Pi*, Tomatillo; *Sp*, winter cherry; *At*, Arabidopsis; *Sl*, tomato; *Nt*, tobacco; *Nb*, *N. benthamiana*; *Hv*, barley; *Zm*, maize; RBCL, Rubisco large subunit. E, Knockdown of *NbALP* and *NbCTB* gene expression in *N. benthamiana* confirms specific labeling. Young plants were inoculated with *TRV::GFP*, *TRV::NbALP*, or *TRV::NbCTB*, and 3 weeks later, proteomes were extracted from the upper leaves from two different plants (hence the duplicate) and labeled with FY01 or JOGDA1. Labeled proteomes were separated on protein gels and analyzed by fluorescence scanning and Coomassie Brilliant Blue staining.

genes and different protein processing in the different species. In general, FY01 and JOGDA1 signals correspond to the signals in the MV202 activity profiles, although MV202 labeling profiles are often too weak to display all the signals. Also, as with Arabidopsis labeling, FY01 signals migrate considerably slower on the protein gel than the presumed MV202-labeled counterparts. Thus, FY01 and JOGDA1 labeling facilitates

the deconvolution of otherwise weak or overlapping and complicated activity profiles generated by MV202 labeling. Notable also is the observation that unspecific labeling by FY01 and JOGDA1 occurs more in leaf extracts of some plants (e.g. Arabidopsis and barley), even though the same amount of protein was labeled.

To independently confirm the selective labeling of ALPs and CTBs in *N. benthamiana*, we silenced aleurain-like protease (*NbALP*; UniProt Q2QFR3) and cathepsin B protease (*NbCTB*; UniProt Q1HER6) in *N. benthamiana* using virus-induced gene silencing. Labeling of leaf extracts of *N. benthamiana* with MV202, FY01, and JOGDA1 causes very similar, overlapping signals, in both unchallenged plants (Fig. 4, A–C) and *Tobacco Rattle Virus* (*TRV*::*GFP*) plants (Fig. 4E). Labeling of leaf extracts from protease-silenced plants, however, revealed that FY01 labeling is only suppressed in *TRV*::*NbALP*, whereas JOGDA1 labeling is only suppressed in *TRV*::*NbCTB* plants (Fig. 4E). These data confirm that, also in *N. benthamiana*, FY01 and JOGDA1 selectively label ALPs and CTBs, respectively. These data illustrate the strength of using selective probes to monitor specific proteases on other plant species.

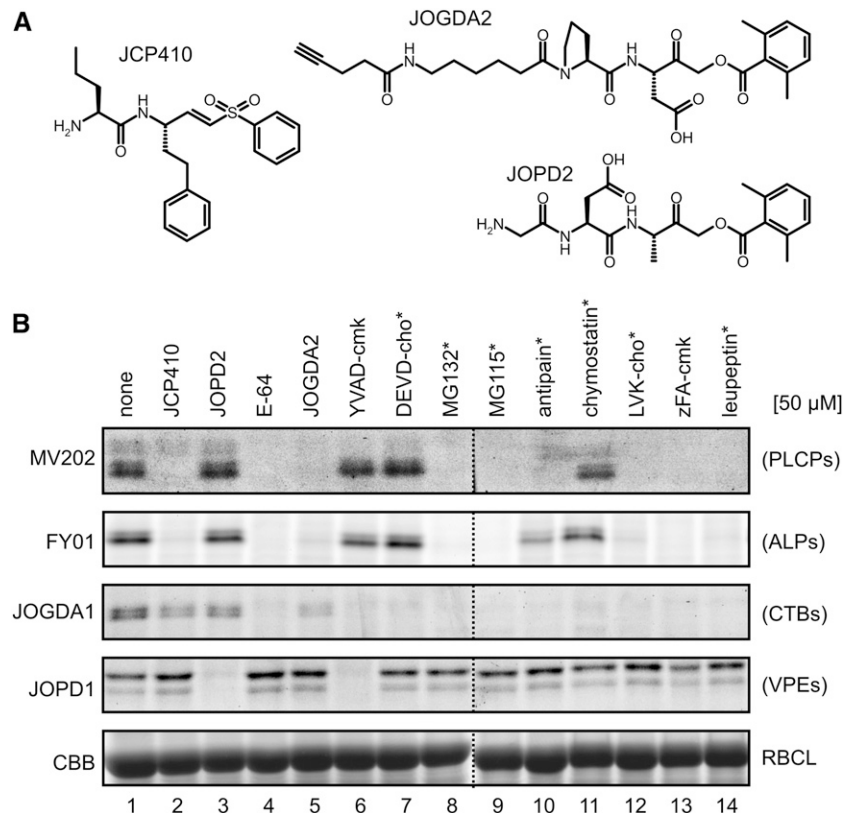
Selective Chemical Interference of Proteases Using Inhibitors

Equipped with the new, selective Cys protease probes, we tested if we could use these probes to

determine the selectivity of commercially available protease inhibitors. We assembled a collection of 13 protease inhibitors that can potentially inhibit Cys proteases. The collection contains caspase inhibitors YVAD-cmk and Asp-Glu-Val-Asp-chloromethylketone (DEVD-cmk), proteasome inhibitors MG132 and MG115, PLCP inhibitors E-64, antipain, chymostatin, and leupeptin, and cathepsin B inhibitors Leu-Val-Lys-aldehyde (LVK-cho) and benzyloxycarbonyl-Phe-Ala-chloromethylketone (zFA-cmk). We also included three custom-made inhibitors (Fig. 5A). JCP410 is an inhibitor of dipeptidyl dipeptidase I/cathepsin C (Arastu-Kapur et al., 2008), consisting of an nor-Val-Phe dipeptide with a vinyl sulfone reactive group, similar to the warhead of the FY01 probe. We also synthesized JOGDA2, which contains a Pro-Asp dipeptide with an AOMK reactive group that is similar to the JOPD1 probe for legumains/VPEs, except that JOGDA2 carries an alkyne minitag instead of the bodipy fluorophore. Finally, we synthesized JOPD2, which consists of a Gly-Asp-Ala tripeptide and an AOMK reactive group, similar to the warhead of the fluorescent FH11 and JOGDA1 probes. All these inhibitors will covalently and irreversibly react with the active-site Cys residues of the proteases, with the exception of the aldehyde-based inhibitors (MG132, MG115, antipain, chymostatin, LVK-cho, and leupeptin), which covalently but reversibly bind to the substrate-binding groove.

Leaf extracts were preincubated with 50 μM of the putative protease inhibitors and then incubated with

Figure 5. Commercial and custom-made protease inhibitors display unexpected specificities. A, Structures of JCP410 and custom-made JOGDA2 and JOPD2. B, Specific protease inhibition by small molecules. Leaf extracts were preincubated for 30 min with 50 μM inhibitors and then labeled with MV202, FY01, JOGDA1, or JOPD1 for 3 h. Labeled proteomes were separated on protein gels and analyzed by fluorescence scanning and Coomassie Brilliant Blue (CBB) staining. RBCL, Rubisco large subunit; *, peptide aldehyde.



the different probes to label the noninhibited enzymes. The labeling profiles revealed a surprising diversity of inhibitory activities. In general, suppression of AALP labeling was consistent between MV202 and FY01 labeling (Fig. 5B). Most importantly, these experiments demonstrate a lack of the presumed selectivity of commercially available inhibitors. Proteasome inhibitors MG132 and MG115 also block both AALP and CTB3 labeling but not VPE labeling (Fig. 5B), consistent with our previous observation that MG132 blocks PLCP activities *in vivo* (Kaschani et al., 2009). In addition, cathepsin B inhibitors LVK-cho and zFA-cmk also block AALP and RD21 labeling but not VPE labeling (Fig. 5B), consistent with previous observations (Gilroy et al., 2007). Likewise, caspase inhibitors YVAD-cmk and DEVD-cho also block CTB3 labeling (Fig. 5B). Importantly, YVAD-cmk but not DEVD-cho also blocks VPE labeling (Fig. 5B), consistent with the notion that VPEs have caspase1 but not caspase3 activity (Hatsugai et al., 2004; Rojo et al., 2004; Misas-Villamil et al., 2013). These data illustrate that commercially available inhibitors with claimed specificity should be used on plants with extreme caution. By contrast, our new custom-made inhibitors indicate the desired selective inhibition: JCP410 selectively blocks AALP labeling, displayed using both MV202 and FY01 (Fig. 5B). Likewise, JOPD2 selectively blocks VPE labeling, displayed with JOPD1 (Fig. 5B). Unexpectedly, JOGDA2 is not selective, as it suppresses AALP labeling in addition to CTB3 labeling (Fig. 5B). Thus, these data indicate that the inhibitors JCP410, DEVD-cho, and JOPD2 can be used for selective inhibition of the activities of AALP, CTB3, and VPEs, respectively.

Dynamic Protease Activities during Seed Germination

Seed germination is an important phase transition for plants that involves the degradation of seed storage proteins, releasing products that are used to build Rubisco and other proteins (Fig. 6A). Notably, the proteases that are active during seed germination and possibly responsible for the conversion of the seed proteome have not been described before. Here, we investigated protease activities during germination of Arabidopsis seeds using our specific fluorescent probes. The conversion of the seed proteome is clearly visible when the proteomes are separated on protein gels (Fig. 6A). The 12S globulins that cause four signals at 25 to 35 kD and two signals at 15 to 20 kD are degraded during germination, while Rubisco large subunit and other proteins appear (Fig. 6A).

The seed extracts were labeled with specific probes to monitor protease activities. FY01 labeling of extracts of germinating seeds revealed no signals in imbibed seeds (day 0) that were blocked upon preincubation with E-64, three signals of 30 kD that appear at day 1 (signal 1), day 2 (signal 2), and day 3 (signal 4), and a weak signal of 40 kD appearing at day 3 (signal 3; Fig. 6B). All these FY01 signals were suppressed upon

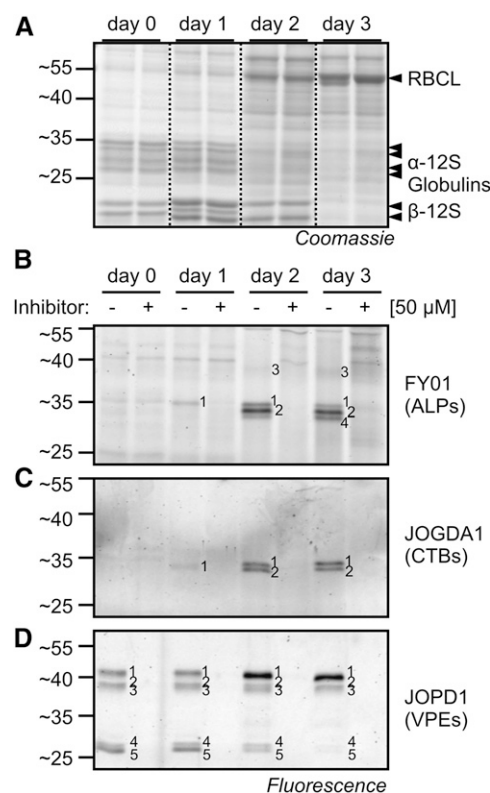


Figure 6. Dynamic protease activities during seed germination. A, Proteome conversion during seed germination. Proteins were extracted from germinating seeds at different time points in duplicate and detected on Coomassie Brilliant Blue-stained protein gels. RBCL, Rubisco large subunit. B to D, Dynamics of protease activities during germination. Protease activities were displayed by labeling protein extracts with FY01 (B), JOGDA1 (C), and JOPD1 (D). For all experiments, seeds were imbibed for 2 d on agar plates at 4°C in the dark and germinated in 16 h of light for 3 d.

preincubation with E-64. JOGDA1 labeling revealed two signals of 30 kD appearing at day 1 (signal 1) and day 2 (signal 2) that were absent upon preincubation with E-64 but no signals in extracts from imbibed seeds (Fig. 6C). Finally, JOPD1 labeling displayed five signals in imbibed seeds in the regions of 40 kD (signals 1–3) and 25 kD (signals 4 and 5), of which signal 1 increases in intensity during seed germination, while signals 4 and 5 decrease in intensity (Fig. 6D). All these JOPD1 signals were absent upon preincubation with YVAD-cmk. These assays illustrate a dynamic change in protease activities during seed germination in Arabidopsis.

Protease Mutants Reveal the Identities of Protease Activities during Seed Germination

We next used protease mutants to annotate the signals in these activity profiles. Importantly, while doing this, we did not detect any alteration in the conversion of seed storage proteins (data not shown),

indicating that none of these proteases is individually essential for seed storage protein degradation.

To identify the FY01 signals during germination, we tested various PLCP mutant seeds. FY01 signals 1, 3, and 4 are absent in the mutants *alp2-1*, *rd21-1*, and *aalp-1*, respectively (Fig. 7A), indicating that they represent ALP2, RD21, and AALP, respectively. Importantly, labeling of RD21 demonstrates that FY01 does not exclusively label ALPs but can incidentally also label other Cys proteases at pH 7. FY01 signal 2 is absent in the *aalp-1* mutant and must be caused by AALP at day 2, but its identity remains unclear at day 3 (Fig. 7A). These data indicate that ALP2 activity appears at day 1 and AALP and RD21 activities appear at day 2. These activities correlate with the transcript levels measured for the corresponding genes during germination (Narsai et al., 2011; Fig. 7B).

We next identified the JOGDA1 signals using single, double, and triple *ctb* mutant seeds. JOGDA1 signal 2 is absent in the *ctb3-1* mutants, indicating that it is caused by CTB3 (Fig. 7C). JOGDA1 signal 1 is also absent in the *ctb3-1* mutant at day 1, indicating that it is caused by CTB3 (Fig. 7C). At later time points, however, signal 1 is reduced in the *ctb3-1* mutant and absent in the *ctb2-1/ctb3-1* double mutants, indicating that this signal consists of CTB2 and CTB3 at days 2 and 3. All signals are absent in the *ctb2-1/ctb3-1* double mutant and the #62-5 triple mutant (Fig. 7C). These data indicate that CTB3 activity appears at day 1 and CTB2 activity follows at day 2. The relative intensities correlate with relative transcript levels: CTB3 is highly expressed, followed by CTB2, whereas CTB1 is poorly expressed (Fig. 7D). More interestingly, CTB2 and CTB3 transcript levels are constitutively high, whereas

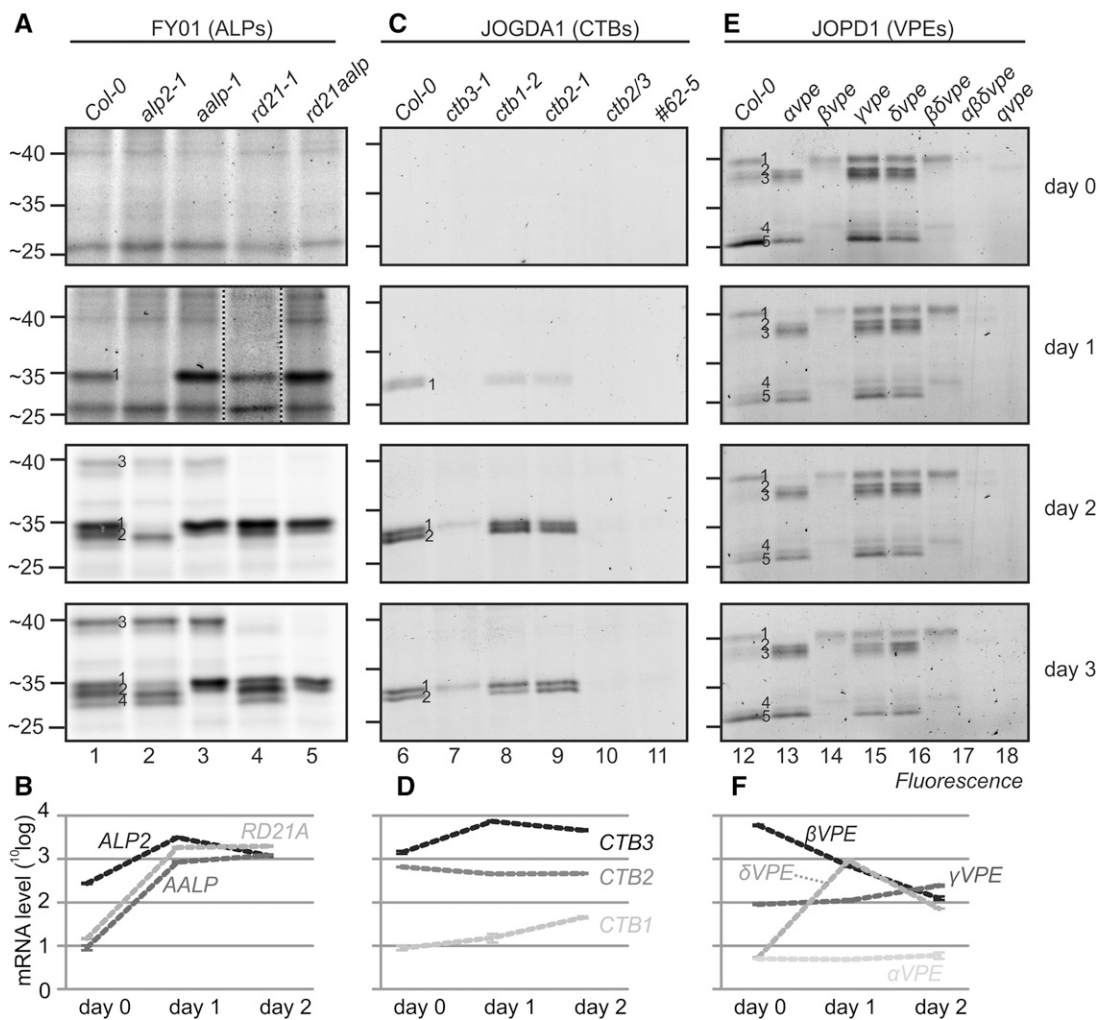


Figure 7. Protease mutants elucidate activity profiles in germinating seeds. A, C, and E, Seeds of wild-type Columbia-0 (Col-0) and protease mutant Arabidopsis plants were imbibed and germinated on plates, and samples were taken at 0, 1, 2, and 3 d post imbibition. Protein extracts of the seeds and seedlings were labeled with FY01 (A), JOGDA1 (C), or JOPD1 (E) at the appropriate conditions, and labeled proteins were detected from protein gels by in-gel fluorescence scanning. B, D, and F, Transcript levels of protease genes in imbibed seeds (day 0) and 1 and 2 d post imbibition. Data were extracted from Narsai et al. (2011).

their activity appears only at 1 and 2 d after imbibition. The absence of CTB activity in the presence of *CTB* transcript indicates that CTBs are subject to post-transcriptional regulation to suppress their activity at early time points.

Finally, we identify the JOPD1 signals using single, double, and triple *vpe* mutant seeds (Gruis et al., 2002, 2004). JOPD1 signal 1 is absent in the αvpe mutant and in the $\alpha\beta\delta vpe$ triple and $qvpe$ quadruple mutants (Fig. 7E), indicating that this signal is caused by αVPE . Signals 2 to 5 are all absent in the βvpe mutant (Fig. 7E), indicating that all these signals are caused by βVPE . Interestingly, there is a weak signal 2 remaining in the βvpe , $\beta\delta vpe$, and $\alpha\beta\delta vpe$ mutants that is absent in the $qvpe$ quadruple mutant (Fig. 7E), indicating that this signal is caused by γVPE . The dominance of βVPE in the JOPD1 activity profile correlates with the fact that the βVPE gene has relatively high transcript levels (Fig. 7F). Surprisingly, however, is the fact that αVPE is clearly detected (Fig. 7E, signal 1), while the αVPE transcript level is relatively low (Fig. 7F). By contrast, γVPE activity is barely detectable (Fig. 7E, signal 2), but the γVPE transcript levels are significantly higher when compared with αVPE (Fig. 7F). The transcript data used here (extracted from Narsai et al., 2011) are consistent with the *VPE* transcript data presented by Gruis et al. (2004). Taken together, these data indicate that there are several cases during seed germination where the activity level of proteases cannot be predicted from the transcript data.

DISCUSSION

Using fluorescent gel imaging and Arabidopsis protease mutants, we have validated the specificity of new fluorescent probes for protease activity profiling in plants. We provide proof of concept on leaf extracts of other plant species and on germinating Arabidopsis seeds. We also used these probes to reveal an unexpected selectivity of commercially available protease inhibitors and found several examples where protease activities do not correspond with transcript levels, highlighting the relevance of this technology to display a new level of functional proteomic information.

The four probes target different Cys proteases at different pH levels. The pH sensitivity is explained by the fact that proteases have pH-dependent activities. Aleurains, for example, show optimal activities at pH 6.5 to 7 (Holwerda and Rogers, 1992), whereas VPEs have an optimal activity at pH 5 (Kuroyanagi et al., 2002). These optimal pH values likely reflect the microenvironment conditions at which these proteases function.

That PLCPs are labeled with MV202 was shown before and is expected, because this probe is based on E-64, which inhibits PLCPs broadly (Richau et al., 2012). Likewise, JOPD1 targets VPEs because they carry an Asp residue at the P1 position, which at low pH is protonated, thereby mimicking an Asn residue

for which VPEs are selective (Kato et al., 2005). The additional P2 = Pro prevents the labeling of PLCPs, which prefer hydrophobic residues at this position. Similar probes carrying a Pro-Asp dipeptide and an AOMK warhead were previously used to label mammalian legumains, which are orthologous to VPEs (Sexton et al., 2007).

Unexpected probe targets were found for FY01 and JOGDA1. FY01 was developed as a specific probe for mammalian cathepsin C, also called dipeptidyl peptidase I (Yuan et al., 2006), but this enzyme does not have a close homolog in plants (Supplemental Fig. S1). Instead, FY01 labels aleurains, which are orthologous to mammalian cathepsin H proteases (Richau et al., 2012; Supplemental Fig. S2). Although slightly unexpected, the selectivity is explained by the fact that aleurains and cathepsin H proteases carry a peptide minichain that blocks part of the substrate-binding groove, thereby preventing endoprotease activity (Guncar et al., 1998). Because of this minichain, the unprimed substrate-binding groove accommodates only two residues, explaining why aleurains cleave two residues from the N terminus and are called aminodipeptidases. Labeling of aleurains by FY01 is explained because FY01 carries two N-terminal residues adjacent to the vinyl sulfone reactive group.

A second unexpected probe target is the selective labeling of CTBs by JOGDA1. JOGDA1 was designed to selectively target AvrPphB by carrying P2 = Asp. This probe should not label PLCPs because they prefer a hydrophobic residue at this position. Surprisingly, our data indicate that, in contrast with other plant PLCPs, CTBs can accommodate acidic residues at the P2 position, hence explaining the selectivity of JOGDA1. Importantly, selective labeling of leaf extracts of other plant species indicated that these properties of ALPs and CTBs are universal, as confirmed by silencing experiments in *N. benthamiana*.

Although FY01 preferentially labels ALPs, we did notice that FY01 also labels 40-kD Cys proteases at lower pH (Fig. 1B) and in seedling extracts (Fig. 7A). This 40-kD signal is probably caused by the labeling of RD21A, as the signal is absent in seedlings of *rd21A-1* mutants. By contrast, JOGDA1 and JOPD1 show selective labeling of CTBs and VPEs, respectively, and we did not detect any labeling of other proteins. Thus, caution is needed for the interpretation of FY01 labeling. To confirm the specificity of labeling, one can (1) knock out/knock down the corresponding protease to show that labeling disappears; (2) purify and identify by mass spectrometry; or (3) characterize labeling further, by studying sensitivity for inhibitors, pH, cofactors, etc. A similar approach was used to characterize VPEs in the apoplast of infected tomato plants (Sueldo et al., 2014).

Besides specific labeling, which can be blocked upon preincubation with a corresponding inhibitor, we also noted strong unspecific labeling of the probes at increasingly high pH. The level of this unspecific labeling is different between the probes and is possibly caused

by the different reactive groups. Epoxide-based MV202 causes strong background labeling at pH 8 to 9, the vinyl sulfone probe FY01 causes background labeling at pH 9, and very low background labeling was displayed by JOGDA1 and JOPD1, which both carry AOMK reactive groups. We also noticed that the intensity of background labeling can depend on the plant species (Fig. 4) and on the type of subcellular extract (data not shown). We have shown that background labeling can be prevented by the precipitation and purification of labeled proteins using probes that carry both a fluorescent group and a biotin affinity handle. We speculate that this unspecific labeling is caused by unspecific labeling of unreacted probes during the heating of the sample in SDS sample buffer.

Using FY01 and JOGDA1 labeling instead of MV202 labeling has several advantages. First, these probes cause much less background labeling and, therefore, are much easier to handle. Second, these probes display different protease classes that are difficult to discriminate by MV202 profiling because of their overlapping molecular mass. This may not be so clear for Arabidopsis leaf extracts, because Arabidopsis AALP and CTB3 have different molecular masses, but this is different for other plant species where the MV202 signals overlap. These studies also readily revealed that monocots may carry multiple CTB isoforms.

Further studies with selective protease probes revealed that commercially available protease inhibitors often have unexpected selectiveness. This is problematic, since many pharmacological studies using these inhibitors in plants have implied the involvement of particular proteases. These conclusions should be carefully reconsidered. Frequently used proteasome inhibitors MG115 and MG132, for example, also inhibit ALPs and CTBs, whereas CTB inhibitors LVK-cho and zFA-cmk also inhibit other PLCPs. However, inhibitors can be remarkably selective for the proteases that we were testing, illustrated by the seeming specific inhibition of ALPs, CTBs, and VPEs by JCP410, DEVD-cho, and JOGDA2, respectively. It should be noted, however, that our data do not exclude that the selective inhibitors also inhibit other proteins that we are not monitoring. More characterized inhibitors can be used for chemical knockout assays to study the role of proteases in plants even if they are not genetic model species.

Protease activity profiling of germinating seeds revealed that the activation of ALPs and CTBs correlates with the remobilization of storage proteins. Although their involvement in seed storage processing seems likely, our data did not demonstrate the involvement of ALPs and CTBs in protein remobilization, because the remobilization is unaltered in the protease mutants and even in the ALP double and CTB triple mutants (data not shown). Redundancy, however, is common for plant proteases, as illustrated by the redundancy of the VPEs in the processing of seed

storage proteins during seed ripening (Shimada et al., 2003; Gruis et al., 2004).

Although some protease activities correlate with transcript levels, others clearly do not. CTB2 and CTB3, for example, are transcribed in seeds, but their activity is undetected until days 1 and 2, indicating that the activities of these CTBs are suppressed at early stages of seed germination. One unconfirmed candidate for CTB regulation is AtCYS6, a cystatin that is expressed in seeds and disappears during germination (Hwang et al., 2009). AtCYS6 knockout mutants germinate faster, indicating a role for AtCYS6 in protease regulation during seed germination (Hwang et al., 2009). It will be interesting to determine if CTB2/3 activities are increased in the AtCYS6 mutants and if AtCYS6 can suppress the labeling of CTB2/3 using competitive activity-based protein profiling (Song et al., 2009; Kaschani et al., 2010; Dong et al., 2014).

We also noted that α VPE causes strong activity signals in germinating seeds, while γ VPE is relatively weak, in contrast to their relative expression levels. This observation indicates that VPE activities are also posttranscriptionally and/or posttranslationally regulated during seed germination, perhaps also through AtCYS6 or AtCYS7, which both carry a C-terminal extension, known to inhibit VPEs (Martinez et al., 2007b). Interestingly, while AtCYS6 is expressed in seeds and disappears during germination, AtCYS7 is coexpressed with γ VPE (Supplemental Fig. S3). A similar posttranslational protease regulation by cystatins has been hypothesized for germinating barley seeds (Martinez et al., 2009). The tight regulation of proteases by cystatins has also been demonstrated in tobacco embryos (Zhao et al., 2013), illustrating the need to monitor these protease activities individually to unravel their functions.

MATERIALS AND METHODS

Activity-Based Probes and Inhibitors

The synthesis of FY01, MV202, and JCP410 has been described before (Yuan et al., 2006; Arastu-Kapur et al., 2008; Richau et al., 2012). The synthesis of JOGDA1, JOPD1, JOGDA2, and JOPD2 is described in Supplemental Text S1. Protease inhibitors E-64, Ac-YVAD-cmk, MG132, MG115, antipain, chymostatin, and leupeptin were purchased from Sigma-Aldrich, and Ac-DEVD-cho, Ac-LVK-cho, and zFA-cmk were purchased from Calbiochem. Synthesized probes and inhibitors are available upon request.

Arabidopsis Mutants

The following Arabidopsis (*Arabidopsis thaliana*) mutants were used in this study: *rd21A-1* (SALK_090550), *aalp-1* (SALK_075550), *ctb3-1* (SALK_019630), *ctb1-2* (SALK_110946; Wang et al., 2008), #62-5 (McLellan et al., 2009), and *acpe*, *brpe*, *γpe*, *δpe*, *βδpe*, *αβδpe*, and *qpe* (Gruis et al., 2004). The *alp2-1* mutant (SALK_079981) and the *ctb2-1* mutant (SALK_089030) were selected for this study using primers flanking the transfer DNA insertion site (5'-TCTGTGCGACTATTGAG-3' and 5'-TTGTGGATCTTGTGGAC-3' 5'-CGTTGGTCACACATAGTGCAG-3' and 5'-GACAATACTGGTTCCTCGCAC-3', respectively) and the LBA1 primer 5'-TGGTTCACGTA-GTGGCCATCG-3'. The *ctb3-1/ctb2-1* double mutant was generated by crossing, and the *rd21-1/aalp-1* double mutant was reported before (Gu et al., 2012). Arabidopsis plants were grown at 22°C (day)/20°C (night) in a

greenhouse under a 16-h light regime. Leaves from rosettes of 6-week-old Arabidopsis plants were used for the protein extraction.

Agroinfiltration

Leaves of *Nicotiana benthamiana* that transiently express proteases were prepared as described before (Richau et al., 2012; Misas-Villamil et al., 2013) using binary plasmids pFK16(35S::CTB3), pFK17(35S::AALP), pHL7(35S::ALP2), pFK137(35S:: α VPE), pFK138(35S:: β VPE), pFK139(35S:: γ VPE), and pFK140 (35S:: δ VPE). pFK16, pFK17, and pFK137 to pFK140 have been described before (Richau et al., 2012; Misas-Villamil et al., 2013). pHL7 was constructed as described before (Shabab et al., 2008) by cloning a PCR fragment amplified using primers 5'-TGCAATCCCAAGTCCCAAC-3' and 5'-AGCTCCATGGCTGTGAAACTAACCTATCTTCCTC-3' from Arabidopsis complementary DNA into pFK26 using *Nco*I and *Pst*I restriction sites, resulting in pHL6. The 35S::ALP2 expression cassette was shuttled from pHL6 into pTP5 using *Xba*I and *Sal*I restriction sites. *Agrobacterium tumefaciens* cultures (optical density = 1) carrying binary plasmid encoding the silencing inhibitor p19 were mixed (1:1) with and without *A. tumefaciens* carrying a binary plasmid encoding the different proteases and agroinfiltrated into expanded leaves of 4-week-old *N. benthamiana* plants. At day 4 after agroinfiltration, six leaf discs (each 1 cm diameter) were ground in 600 μ L of extraction buffer containing 1% (w/v) polyvinylpyrrolidone and 2 mM dithiothreitol (DTT). The pH of the extraction buffer was pH 5 (for VPEs), pH 6 (for CTBs), or pH 7 (for ALPs). The extract was cleared by centrifugation, and the supernatant was preincubated for 30 min with or without 50 μ M E-64 or YVAD-cmk and labeled for 4 h with 2 μ M of the respective probe. Labeled proteins were detected by in-gel fluorescence scanning.

Other Plant Species

Other plant species were grown under normal greenhouse conditions, and samples were taken from adult, expanded leaves. Proteins were extracted in 2 mM DTT. For *N. benthamiana* and tobacco (*Nicotiana tabacum*), 5% (w/v) polyvinylpyrrolidone was added before protein extractions. Protein concentrations were measured and normalized before labeling.

Virus-Induced Gene Silencing

TRV::NbALP and *TRV::NbCTB* were generated by cloning a 300-bp fragment of NbS0032309g0011.1 (*NbALP*) and NbS00035145g0007.1 (*NbCTB*) using primers 5'-GATCGGATCCGAGGTACGAGACAGTTGAGGAG-3', 5'-GATCGAATTCAGCAAGATCCGCACTTGCCCTGG-3', 5'-GATCGGATCCGGCCGATGGAAAGCTGCACTG-3', and 5'-GATCGAATTCCTGCTGACAGAGAGATATCAAGCC-3', resulting in pTS9 (*TRV::NbALP*) and pTS7 (*TRV::NbCTB*), respectively. Overnight-grown *A. tumefaciens* cultures (strain GV3101) carrying plasmids pTS7 and pTS9 were resuspended in infiltration buffer (10 mM MES, pH 5, 10 mM MgCl₂, and 1 mM acetosyringone). The optical density at 600 nm was adjusted to 2, and cultures carrying pTS7 and pTC9 were mixed with cultures carrying the *TRV1* vector. Cultures were incubated for 3 h at room temperature in the dark and infiltrated into the first two true leaves of 2-week-old *N. benthamiana* plants. Total proteins were extracted from upper leaves after 3 weeks and used for labeling.

Seed Germination

Arabidopsis seeds were sterilized and plated on one-half-strength Murashige and Skoog (MS) medium (2.15 g L⁻¹ MS medium; Duchefa M0221) containing 1% (w/v) agar. Seeds were imbibed on one-half-strength MS agar plates for 2 d at 4°C in the dark. The agar plates were incubated at 20°C to 22°C under a 16-h light regime for seed germination. Seeds were collected at days 0, 1, 2, and 3 post imbibition and frozen at -80°C until protein extraction.

Leaf Protein Extraction and Labeling

A total of 600 μ L of extraction buffer containing 50 mM sodium acetate (for pH 6 and below) or 50 mM Tris-HCl (for pH 7 and above) and 2 mM DTT were added to six leaf discs (1 cm diameter) of Arabidopsis in a 1.5-mL tube. After grinding the tissues with a plastic blue stick, the samples were centrifuged at 10,000g and 4°C for 10 min, and the supernatant containing the soluble proteins was used for labeling. Labeling was performed in a 50- μ L total volume.

A total of 45 μ L of leaf extracts (containing approximately 100 μ g of soluble proteins) was preincubated with 50 μ M E-64 or Ac-YVAD-cmk for 30 min at room temperature. These extracts were incubated with 2 μ M MV202 or JOPD1, 0.06 μ M FY01, or 5 μ M JOGDA1 for 4 h at room temperature in the dark. Equal volumes of dimethyl sulfoxide (DMSO) were added for no-probe controls.

Seed Protein Extraction and Labeling

Proteins were extracted by grinding the seeds in sterilized water. The samples were centrifuged at 10,000g and 4°C for 10 min, and the supernatant containing the soluble proteins was used for labeling. Labeling was performed in a 50- μ L format. A total of 45 μ L of seed extracts (containing approximately 50 μ g of soluble proteins) was preincubated with 50 μ M E-64 at pH 6 (MV202 or JOGDA1) or pH 7 (FY01) or 50 μ M Ac-YVAD-cmk at pH 5 (JOPD1) or DMSO for 30 min at room temperature. These extracts were incubated with 2 μ M FY01, JOGDA1, or JOPD1 for 4 h at room temperature in the dark. Equal volumes of DMSO were added to the no-probe control.

Improved MV202 Labeling

A total of 50 to 100 μ g of leaf extract was preincubated with or without 50 μ M E-64 (or other commercial protease inhibitors) in a 500- μ L total volume containing 50 mM Tris (pH 6) and 2 mM DTT at room temperature for 30 min, then 1 μ L of 1 mM MV202 (or DCG-04) was added. The samples were kept on the rotator in the dark at room temperature for 4 h. The samples were precipitated by adding 1 mL of ice-cold acetone, centrifuging at 4°C at 10,000g for 5 min, and washing with 70% (v/v) cold acetone once. Protein pellets were resuspended in 50 mM Tris-HCl (pH 7) containing 10 μ L of avidin agarose (Sigma-Aldrich) beads. Samples were incubated with the beads at room temperature for 1 h, and the beads were washed with 1% (w/v) SDS twice and heated for 5 min at 95°C in 50 μ L of SDS gel-loading buffer.

Analysis of Labeled Proteins

The labeling reactions were stopped by adding gel-loading buffer containing β -mercaptoethanol at 1 \times final concentration and heating at 95°C for 5 min. The labeled proteins were separated on 12% (v/v) protein gels at 200 V for 1 h. The labeled proteins were detected from the protein gels with a Typhoon FLA 9400 scanner (Amersham Biosciences/GE Healthcare) using an excitation wavelength of 532 nm and a 580-nm band-pass filter (580BP30).

Bioinformatics

Transcript levels published by Narsai et al. (2011) were extracted from the National Center for Biotechnology Information Gene Expression Omnibus data set GSE30223 using GEO2R. The phylogenetic trees of human PLCPs (Lecaille et al., 2002) and Arabidopsis PLCPs (Richau et al., 2012) were made by Cluster Omega (Sievers et al., 2011).

Supplemental Data

The following supplemental materials are available.

Supplemental Figure S1. Accumulation and labeling of RD21 in *ctb3-1* mutant plants.

Supplemental Figure S2. Phylogenetic tree of human and Arabidopsis PLCPs.

Supplemental Figure S3. Coexpression of *ATCYS6* with γ VPE during development.

Supplemental Text S1. Chemical synthesis of AOMK probes.

ACKNOWLEDGMENTS

We thank Hermen Overkleeft and Martijn Verdoes for providing MV202 and DCG-04, Leonard Both for mining Genevestigator data, and Adriana Pruzinska for technical assistance.

Received November 26, 2014; accepted May 27, 2015; published June 5, 2015.

LITERATURE CITED

- Ahmed SU, Rojo E, Kovaleva V, Venkataraman S, Dombrowski JE, Matsuoka K, Raikhel NV (2000) The plant vacuolar sorting receptor AtELP is involved in transport of NH(2)-terminal propeptide-containing vacuolar proteins in *Arabidopsis thaliana*. *J Cell Biol* **149**: 1335–1344
- Arastu-Kapur S, Ponder EL, Fonović UP, Yeoh S, Yuan F, Fonović M, Grainger M, Phillips CI, Powers JC, Bogyo M (2008) Identification of proteases that regulate erythrocyte rupture by the malaria parasite *Plasmodium falciparum*. *Nat Chem Biol* **4**: 203–213
- Beers EP, Jones AM, Dickerman AW (2004) The S8 serine, C1A cysteine and A1 aspartic protease families in *Arabidopsis*. *Phytochemistry* **65**: 43–58
- Bozkurt TO, Schornack S, Win J, Shindo T, Ilyas M, Oliva R, Cano LM, Jones AM, Huitema E, van der Hoorn RA, et al (2011) *Phytophthora infestans* effector AVRblb2 prevents secretion of a plant immune protease at the haustorial interface. *Proc Natl Acad Sci USA* **108**: 20832–20837
- Dong S, Stam R, Cano LM, Song J, Sklenar J, Yoshida K, Bozkurt TO, Oliva R, Liu Z, Tian M, et al (2014) Effector specialization in a lineage of the Irish potato famine pathogen. *Science* **343**: 552–555
- Eason JR, Ryan DJ, Watson LM, Hedderley D, Christey MC, Braun RH, Coupe SA (2005) Suppression of the cysteine protease, aleurain, delays floret senescence in *Brassica oleracea*. *Plant Mol Biol* **57**: 645–657
- García-Lorenzo M, Sjödin A, Jansson S, Funk C (2006) Protease gene families in *Populus* and *Arabidopsis*. *BMC Plant Biol* **6**: 30
- Gilroy EM, Hein I, van der Hoorn R, Boevink PC, Venter E, McLellan H, Kaffarnik F, Hrubikova K, Shaw J, Holeva M, et al (2007) Involvement of cathepsin B in the plant disease resistance hypersensitive response. *Plant J* **52**: 1–13
- Gruis D, Schulze J, Jung R (2004) Storage protein accumulation in the absence of the vacuolar processing enzyme family of cysteine proteases. *Plant Cell* **16**: 270–290
- Gruis DF, Selinger DA, Curran JM, Jung R (2002) Redundant proteolytic mechanisms process seed storage proteins in the absence of seed-type members of the vacuolar processing enzyme family of cysteine proteases. *Plant Cell* **14**: 2863–2882
- Gu C, Shabab M, Strasser R, Wolters PJ, Shindo T, Niemer M, Kaschani F, Mach L, van der Hoorn RA (2012) Post-translational regulation and trafficking of the granulin-containing protease RD21 of *Arabidopsis thaliana*. *PLoS ONE* **7**: e32422
- Guncar G, Podobnik M, Pungercar J, Strukelj B, Turk V, Turk D (1998) Crystal structure of porcine cathepsin H determined at 2.1 Å resolution: location of the mini-chain C-terminal carboxyl group defines cathepsin H aminopeptidase function. *Structure* **6**: 51–61
- Haedke U, Küttler EV, Vosyko O, Yang Y, Verhelst SHL (2013) Tuning probe selectivity for chemical proteomics applications. *Curr Opin Chem Biol* **17**: 102–109
- Hao L, Hsiang T, Goodwin PH (2006) Role of two cysteine proteinases in the susceptible response of *Nicotiana benthamiana* to *Colletotrichum destructivum* and the hypersensitive response to *Pseudomonas syringae* pv. *tomato*. *Plant Sci* **170**: 1001–1009
- Hatsugai N, Kuroyanagi M, Yamada K, Meshi T, Tsuda S, Kondo M, Nishimura M, Hara-Nishimura I (2004) A plant vacuolar protease, VPE, mediates virus-induced hypersensitive cell death. *Science* **305**: 855–858
- Heal WP, Dang TH, Tate EW (2011) Activity-based probes: discovering new biology and new drug targets. *Chem Soc Rev* **40**: 246–257
- Holwerda BC, Rogers JC (1992) Purification and characterization of aleurain: a plant thiol protease functionally homologous to mammalian cathepsin H. *Plant Physiol* **99**: 848–855
- Hörger AC, Ilyas M, Stephan V, Tellier A, van der Hoorn RA, Rose LE (2012) Balancing selection at the tomato RCR3 Guardee gene family maintains variation in strength of pathogen defense. *PLoS Genet* **8**: e1002813
- Hwang JE, Hong JK, Je JH, Lee KO, Kim DY, Lee SY, Lim CO (2009) Regulation of seed germination and seedling growth by an *Arabidopsis* phytocystatin isoform, AtCYS6. *Plant Cell Rep* **28**: 1623–1632
- Kaschani F, Shabab M, Bozkurt T, Shindo T, Schornack S, Gu C, Ilyas M, Win J, Kamoun S, van der Hoorn RA (2010) An effector-targeted protease contributes to defense against *Phytophthora infestans* and is under diversifying selection in natural hosts. *Plant Physiol* **154**: 1794–1804
- Kaschani F, Verhelst SH, van Swieten PF, Verdoes M, Wong CS, Wang Z, Kaiser M, Overkleeft HS, Bogyo M, van der Hoorn RA (2009) Minitags for small molecules: detecting targets of reactive small molecules in living plant tissues using ‘click chemistry’. *Plant J* **57**: 373–385
- Kato D, Boatright KM, Berger AB, Nazif T, Blum G, Ryan C, Chehade KA, Salvesen GS, Bogyo M (2005) Activity-based probes that target diverse cysteine protease families. *Nat Chem Biol* **1**: 33–38
- Krüger J, Thomas CM, Golstein C, Dixon MS, Smoker M, Tang S, Mulder L, Jones JD (2002) A tomato cysteine protease required for Cf-2-dependent disease resistance and suppression of autonecrosis. *Science* **296**: 744–747
- Kuroyanagi M, Nishimura M, Hara-Nishimura I (2002) Activation of *Arabidopsis* vacuolar processing enzyme by self-catalytic removal of an auto-inhibitory domain of the C-terminal propeptide. *Plant Cell Physiol* **43**: 143–151
- Kuroyanagi M, Yamada K, Hatsugai N, Kondo M, Nishimura M, Hara-Nishimura I (2005) Vacuolar processing enzyme is essential for mycotoxin-induced cell death in *Arabidopsis thaliana*. *J Biol Chem* **280**: 32914–32920
- Lampl N, Alkan N, Davydov O, Fluhr R (2013) Set-point control of RD21 protease activity by AtSerpin1 controls cell death in *Arabidopsis*. *Plant J* **74**: 498–510
- Lampl N, Budai-Hadrian O, Davydov O, Joss TV, Harrop SJ, Curmi PMG, Roberts TH, Fluhr R (2010) *Arabidopsis* AtSerpin1, crystal structure and in vivo interaction with its target protease RESPONSIVE TO DESICCATION-21 (RD21). *J Biol Chem* **285**: 13550–13560
- Lecaille F, Kaleta J, Brömme D (2002) Human and parasitic papain-like cysteine proteases: their role in physiology and pathology and recent developments in inhibitor design. *Chem Rev* **102**: 4459–4488
- Lozano-Torres JL, Wilbers RH, Gawronski P, Boshoven JC, Finkers-Tomczak A, Cordewener JH, America AH, Overmars HA, Van't Klooster JW, Baranowski L, et al (2012) Dual disease resistance mediated by the immune receptor Cf-2 in tomato requires a common virulence target of a fungus and a nematode. *Proc Natl Acad Sci USA* **109**: 10119–10124
- Lu H, Wang Z, Shabab M, Oeljeklaus J, Verhelst SH, Kaschani F, Kaiser M, Bogyo M, van der Hoorn RA (2013) A substrate-inspired probe monitors translocation, activation, and subcellular targeting of bacterial type III effector protease AvrPphB. *Chem Biol* **20**: 168–176
- Martínez DE, Bartoli CG, Grbic V, Guíamet JJ (2007a) Vacuolar cysteine proteases of wheat (*Triticum aestivum* L.) are common to leaf senescence induced by different factors. *J Exp Bot* **58**: 1099–1107
- Martínez M, Cambra I, Carrillo L, Díaz-Mendoza M, Díaz I (2009) Characterization of the entire cystatin gene family in barley and their target cathepsin L-like cysteine-proteases, partners in the hordein mobilization during seed germination. *Plant Physiol* **151**: 1531–1545
- Martínez M, Cambra I, González-Melendi P, Santamaría ME, Díaz I (2012) C1A cysteine-proteases and their inhibitors in plants. *Physiol Plant* **145**: 85–94
- Martínez M, Díaz-Mendoza M, Carrillo L, Díaz I (2007b) Carboxy terminal extended phytocystatins are bifunctional inhibitors of papain and legumain cysteine proteinases. *FEBS Lett* **581**: 2914–2918
- McLellan H, Gilroy EM, Yun BW, Birch PR, Loake GJ (2009) Functional redundancy in the *Arabidopsis* cathepsin B gene family contributes to basal defence, the hypersensitive response and senescence. *New Phytol* **183**: 408–418
- Misas-Villamil JC, Toenges G, Kolodziejek I, Sadaghiani AM, Kaschani F, Colby T, Bogyo M, van der Hoorn RA (2013) Activity profiling of vacuolar processing enzymes reveals a role for VPE during oomycete infection. *Plant J* **73**: 689–700
- Mueller AN, Ziemann S, Treitschke S, Aßmann D, Doehlemann G (2013) Compatibility in the *Ustilago maydis*-maize interaction requires inhibition of host cysteine proteases by the fungal effector Pit2. *PLoS Pathog* **9**: e1003177
- Nakaune S, Yamada K, Kondo M, Kato T, Tabata S, Nishimura M, Hara-Nishimura I (2005) A vacuolar processing enzyme, δ VPE, is involved in seed coat formation at the early stage of seed development. *Plant Cell* **17**: 876–887
- Narsai R, Law SR, Carrie C, Xu L, Whelan J (2011) In-depth temporal transcriptome profiling reveals a crucial developmental switch with roles for RNA processing and organelle metabolism that are essential for germination in *Arabidopsis*. *Plant Physiol* **157**: 1342–1362
- Richau KH, Kaschani F, Verdoes M, Pansuriya TC, Niessen S, Stüber K, Colby T, Overkleeft HS, Bogyo M, Van der Hoorn RA (2012) Sub-classification and biochemical analysis of plant papain-like cysteine

- proteases displays subfamily-specific characteristics. *Plant Physiol* **158**: 1583–1599
- Royo E, Martín R, Carter C, Zouhar J, Pan S, Plotnikova J, Jin H, Paneque M, Sánchez-Serrano JJ, Baker B, et al** (2004) VPEgamma exhibits a caspase-like activity that contributes to defense against pathogens. *Curr Biol* **14**: 1897–1906
- Rooney HC, Van't Klooster JW, van der Hoorn RA, Joosten MH, Jones JD, de Wit PJ** (2005) *Cladosporium Avr2* inhibits tomato Rcr3 protease required for Cf-2-dependent disease resistance. *Science* **308**: 1783–1786
- Serim S, Haedke U, Verhelst SH** (2012) Activity-based probes for the study of proteases: recent advances and developments. *ChemMedChem* **7**: 1146–1159
- Sexton KB, Witte MD, Blum G, Bogyo M** (2007) Design of cell-permeable, fluorescent activity-based probes for the lysosomal cysteine protease asparaginyl endopeptidase (AEP)/legumain. *Bioorg Med Chem Lett* **17**: 649–653
- Shabab M, Shindo T, Gu C, Kaschani F, Pansuriya T, Chinthra R, Harzen A, Colby T, Kamoun S, van der Hoorn RA** (2008) Fungal effector protein AVR2 targets diversifying defense-related Cys proteases of tomato. *Plant Cell* **20**: 1169–1183
- Shimada T, Yamada K, Kataoka M, Nakaune S, Koumoto Y, Kuroyanagi M, Tabata S, Kato T, Shinozaki K, Seki M, et al** (2003) Vacuolar processing enzymes are essential for proper processing of seed storage proteins in *Arabidopsis thaliana*. *J Biol Chem* **278**: 32292–32299
- Shindo T, Misas-Villamil JC, Hörger AC, Song J, van der Hoorn RA** (2012) A role in immunity for *Arabidopsis* cysteine protease RD21, the ortholog of the tomato immune protease C14. *PLoS ONE* **7**: e29317
- Sievers F, Wilm A, Dineen D, Gibson TJ, Karplus K, Li W, Lopez R, McWilliam H, Remmert M, Söding J, et al** (2011) Fast, scalable generation of high-quality protein multiple sequence alignments using Clustal Omega. *Mol Syst Biol* **7**: 539
- Song J, Win J, Tian M, Schornack S, Kaschani F, Ilyas M, van der Hoorn RAL, Kamoun S** (2009) Apoplastic effectors secreted by two unrelated eukaryotic plant pathogens target the tomato defense protease Rcr3. *Proc Natl Acad Sci USA* **106**: 1654–1659
- Sueldo D, Ahmed A, Misas-Villamil J, Colby T, Tameling W, Joosten MH, van der Hoorn RA** (2014) Dynamic hydrolase activities precede hypersensitive tissue collapse in tomato seedlings. *New Phytol* **203**: 913–925
- Tian M, Win J, Song J, van der Hoorn R, van der Knaap E, Kamoun S** (2007) A *Phytophthora infestans* cystatin-like protein targets a novel tomato papain-like apoplastic protease. *Plant Physiol* **143**: 364–377
- van der Hoorn RA** (2008) Plant proteases: from phenotypes to molecular mechanisms. *Annu Rev Plant Biol* **59**: 191–223
- van der Hoorn RA, Leeuwenburgh MA, Bogyo M, Joosten MH, Peck SC** (2004) Activity profiling of papain-like cysteine proteases in plants. *Plant Physiol* **135**: 1170–1178
- van der Linde K, Hemetsberger C, Kastner C, Kaschani F, van der Hoorn RA, Kumlehn J, Doehlemann G** (2012) A maize cystatin suppresses host immunity by inhibiting apoplastic cysteine proteases. *Plant Cell* **24**: 1285–1300
- van Esse HP, Van't Klooster JW, Bolton MD, Yadeta KA, van Baarlen P, Boeren S, Vervoort J, de Wit PJ, Thomma BP** (2008) The *Cladosporium fulvum* virulence protein Avr2 inhibits host proteases required for basal defense. *Plant Cell* **20**: 1948–1963
- Wang Z, Gu C, Colby T, Shindo T, Balamurugan R, Waldmann H, Kaiser M, van der Hoorn RA** (2008) Beta-lactone probes identify a papain-like peptide ligase in *Arabidopsis thaliana*. *Nat Chem Biol* **4**: 557–563
- Willems LI, Overkleef HS, van Kasteren SI** (2014) Current developments in activity-based protein profiling. *Bioconjug Chem* **25**: 1181–1191
- Yuan F, Verhelst SH, Blum G, Coussens LM, Bogyo M** (2006) A selective activity-based probe for the papain family cysteine protease dipeptidyl peptidase I/cathepsin C. *J Am Chem Soc* **128**: 5616–5617
- Zhang D, Liu D, Lv X, Wang Y, Xun Z, Liu Z, Li F, Lu H** (2014) The cysteine protease CEP1, a key executor involved in tapetal programmed cell death, regulates pollen development in *Arabidopsis*. *Plant Cell* **26**: 2939–2961
- Zhao P, Zhou XM, Zhang LY, Wang W, Ma LG, Yang LB, Peng XB, Bozhkov PV, Sun MX** (2013) A bipartite molecular module controls cell death activation in the basal cell lineage of plant embryos. *PLoS Biol* **11**: e1001655
- Zulet A, Gil-Monreal M, Villamor JG, Zabalza A, van der Hoorn RA, Royuela M** (2013) Proteolytic pathways induced by herbicides that inhibit amino acid biosynthesis. *PLoS ONE* **8**: e73847